DOI: 10.26599/FSHW.2025.9250869

Contents lists available at SciOpen

Food Science and Human Wellness

journal homepage: https://www.sciopen.com/journal/2097-0765

China Food Publishing Co.

Transcriptomic insights into the synergistic bactericidal mechanisms of the simultaneous treatment of ultrasound and ultraviolet on *Escherichia coli* O157:H7

Qin Li [a], Yuhao Wu [a], Yi Chen [a], Jianwei Zhou [b], Donghong Liu [a, c], Ruiling Lv[a, c, *]

[a] *Ningbo Global Innovation Center, Zhejiang University, Ningbo 315100, China*

[b] *NingboTech University, Ningbo 315100, China*

[c] *College of Biosystems Engineering and Food Science, National-Local Joint Engineering Laboratory of Intelligent Food Technology and Equipment, Fuli Institute of Food Science, Zhejiang University, Hangzhou 310058, China*

ABSTRACT: This study analyzed the differentially expressed genes (DEGs) of *Escherichia coli* O157:H7 after combined ultrasound and ultraviolet (US+UV) treatment to explore molecular inactivation mechanisms. A total of 2,133 genes showed differential expression, including 1,055 up-regulated and 1,078 down-regulated genes, indicating pronounced transcriptomic changes. Functional enrichment analyses based on Gene Ontology (GO) and the Kyoto Encyclopedia of Genes and Genomes (KEGG) databases demonstrated that these DEGs were mainly associated with pathways related to carbohydrate metabolism and transport, the tricarboxylic acid (TCA) cycle, amino acid synthesis, oxidative phosphorylation, and quorum sensing. Notably, TCA cycle-related genes (*frdD*, *frdB*) were significantly up-regulated, which likely enhanced electron flow into the oxidative phosphorylation pathway, thereby promoting ATP synthesis and energy production to counteract stress-induced damage. Conversely, genes related to ABC transporters (e.g., *fepB*, *malK*) and ribosomal proteins (e.g., *rplK*, *rpsF*) were markedly down-regulated, indicating that disrupted membrane transport and protein synthesis under stress conditions. Furthermore, the up-regulation of quorum sensing genes (e.g., *lsrC*, *lsrK*) indicated enhanced intercellular communication, possibly linked to stress adaptation. Overall, US+UV treatment exerted a profound impact on multiple metabolic and regulatory pathways, leading to cellular dysfunction and potentially cell death. The study provided valuable mechanistic insights into the synergistic bactericidal effects of non-thermal US+UV treatment and offered a molecular basis for its application in food safety interventions.

Keywords: Ultrasound treatment; Ultraviolet; Transcriptomic analysis; inactivation effect; Non-thermal processing;

1. Introduction

Ultrasound (US) technology, as a non-thermal sterilization method, effectively inactivates microorganisms while preserving the original flavor, nutritional components, and color of food. Additionally, ultrasound equipment is simple in design, environmentally friendly, and easily automated[1]. Ultrasound technology has shown significant effectiveness in eliminating common foodborne pathogens, namely *Escherichia coli* (*E. coli*) and *Salmonella*, which are major causes of foodborne illness. By

***Corresponding author**
lvruiling@zju.edu.cn.

Received 8 July 2025
Received in revised from 6 August 2025
Accepted 28 August 2025

disturbing bacterial membranes and cell walls, ultrasound waves induce the release of intracellular contents, ultimately causing bacterial death[2]. The bactericidal effect of ultrasound relies not only on its mechanical physical effects but also on its thermal effects, as the localized heat generated by the sound wave vibrations further accelerates bacterial inactivation. Ultrasound achieves microbial inactivation through dual mechanisms, enabling safe food sterilization without chemicals and simultaneously preserving taste, texture, and nutritional integrity [3].

However, its standalone bactericidal effect is often suboptimal, and there is a potential risk of cross-contamination, which must be carefully considered in practical applications. In contrast, conventional thermal sterilization effectively eliminates most pathogenic and spoilage microorganisms, enhancing food safety [4]. However, high-temperature treatment may degrade nutritional and sensory qualities and is energy-intensive [5]. To optimize sterilization efficacy while preserving food quality and maximizing energy and cost efficiency, the potential of ultrasound as a non-thermal sterilization method has been widely explored, particularly in combination with technologies such as ultraviolet (UV) irradiation, high-pressure processing, and pulsed electric fields. Notably, the synergistic interaction between ultrasound and UV has been shown to significantly enhance the inactivation efficacy against *E. coli* O157:H7[6]. The US+UV treatment exhibited a stronger bactericidal effect against *E. coli* O157:H7 than either treatment alone. This finding was consistent with recent research by Chen et al. [7], who demonstrated that the combined application of ultrasound and UV resulted in a greater than 7 Log CFU/mL reduction in *E. coli* O157:H7 within 40 seconds. In contrast, ultrasound alone produced only marginal reductions in bacterial counts, and UV alone achieved a reduction of approximately 2.00 Log CFU/mL under similar conditions.

When exposed to external physical stresses such as US and UV irradiation, microorganisms are often capable of maintaining genomic integrity and essential physiological functions. However, these external stressors may significantly impact gene expression patterns, potentially altering cellular physiological responses and adaptive mechanisms. To elucidate the fundamental molecular mechanisms underlying stress-induced phenotypic variation in microorganisms, transcriptomic and genomic approaches have been increasingly employed to analyze differentially expressed genes (DEGs) under various treatment conditions. Such molecular-level analyses are instrumental in identifying key regulatory genes and signaling pathways involved in stress responses and in advancing our understanding of microbial adaptation to adverse environmental conditions. Previous studies reported the efficacy of non-thermal sterilization technologies on microorganisms at the molecular level. For instance, Mareike et al.[8] investigated the bactericidal activity of non-thermal atmospheric pressure plasma in liquid environments on *Pseudomonas aeruginosa*, and further explored its disruptive effects on microbial membranes at the molecular level. Similarly, Wen et al.[9] conducted a metabolomics-based study and performed genome sequencing of *E. coli* and *Staphylococcus aureus*, systematically elucidating the antimicrobial mechanism of thymol against foodborne pathogens and validating their findings through functional analyses.

To further explore the microbial response mechanisms to multiple external stressors—including photonic stress, plasma treatment, high-pressure processing, and UV exposure—gene expression microarray technologies have been employed to compare gene expression profiles under different stress conditions. With the rapid advancement of high-throughput sequencing technologies, Next-Generation Sequencing (NGS) has emerged as a superior alternative to conventional microarray platforms, offering genome-wide transcriptomic profiling with greater sensitivity, accuracy, and reduced false discovery rates. NGS enables researchers not only to obtain a broader gene expression landscape but also to gain insights into gene regulatory networks, alternative splicing, mutations, transcription start sites, and other genomic features, thereby propelling research in molecular biology and functional genomics. For example, studies by Al-Jassim[10] and Zhao[11] examined gene expression changes in *E. coli* under solar irradiation and high-pressure carbon dioxide treatments, respectively, using RNA-seq to uncover the molecular impacts of these non-thermal sterilization techniques.

This study sought to investigate the impact of combined US and UV treatment on *E. coli* O157:H7 by analyzing gene expression profiles through transcriptomic approaches. By identifying key DEGs and their involvement in major metabolic pathways, this research sought to uncover the molecular mechanisms underlying the bactericidal effects of the combined treatment and to deepen our understanding of the associated changes in microbial biological functions.

2. Materials and methods

2.1 Materials and chemicals

The *E. coli* O157:H7 was purchased from BeNa Culture Collection Biotechnology Co., Ltd. TRIzol® reagent, TURBO DNA-free™ kit, SuperScript IV reverse transcriptase and messenger RNA (mRNA) purification kit were purchased from Thermo Fisher Scientific Inc. The complementary DNA (cDNA) synthesis kit and the BIOG^{HC} Elitefast SYBR kit were purchased from Changzhou Bio-generating Biotechnology Corp (BIOG). Ribonuclease H (RNase H), DNA Polymerase I (*E. coli*) and UltraPure polymerase chain reaction (PCR) deoxynucleotide mix were purchased from Takara Biomedical Technology (Beijing) Co., Ltd. All other chemicals and solvents were of analytical reagent grade and purchased from Beijing Solarbio Science & Technology Co., Ltd.

2.2 Preparation of E. coli suspension

The original bacterial culture of *E. coli* O157:H7 was placed in nutritive meat broth medium (NB medium) containing 50% glycerol and was frozen at -80℃ for long-term storage. Before the experiment, 10 μL of the bacteria was inoculated onto eosin-methylene blue medium (EMB medium) and single colonies were screened by the streaking method. Then, the selected single colonies were transferred to NB medium and cultured at 37℃ and 150 r/min on a shaker for 18 hours until the bacterial strain entered the stable growth phase. During the experiment, the bacterial suspension was diluted to a concentration of approximately 8 log CFU/mL and placed in a quartz beaker for standby.

2.3 Ultrasound and ultraviolet processing

The schematic diagram of the experimental setup was shown in Figure 1. An ultrasound processor (SCIENTZ-IID, Ningbo Scientz Biotechnology Co., Ltd.) and an ultraviolet lamp tube (CZ3457, Royal Philips) were employed. During the research, the ultrasound output power was consistently set at 200 W with a frequency of 20 kHz, while the ultraviolet power was 8 W, with a wavelength of 253.7 nm and an irradiation distance of 6 cm. A volume of 50 mL of the diluted bacterial suspension, at a concentration of 8 Log CFU/mL, was transferred into a 100 mL quartz beaker. The beaker was placed in the acoustic enclosure of the ultrasound processor, with the ultrasound probe submerged to the center depth of the solution. The lamp tube and the processor were turned on at the same time. The combined treatment time was 40 seconds, while the pulse duration and the intermittent duration were set at 2 seconds each.

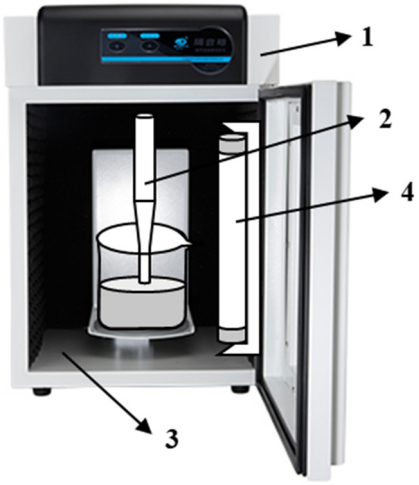

Fig.1 The schematic diagram of the experimental setup (1. ultrasound processor; 2. ultrasound probe; 3. acoustic enclosure; 4. ultraviolet lamp tube).

2.4 Extraction of total RNA from E. coli O157:H7

Total RNA was extracted from both control and treatment groups of *E. coli* O157:H7 using the TRIzol method. To ensure the purity of the extracted RNA, residual DNA contamination was removed using DNase enzyme treatment. The purity of the RNA was assessed by measuring the OD260/280 ratio using a micro volume UV/Vis spectrophotometers (NanoDrop, Thermo Fisher Scientific Inc.) ensuring the absence of protein and other contaminants. Subsequently, RNA concentration and integrity were accurately determined using the bioanalyzer instrument (Agilent 2100, Agilent Technologies Inc.) to guarantee the acquisition of high-quality RNA samples for downstream analyses.

2.5 Construction of cDNA library

Following the confirmation of RNA sample quality, bacterial mRNA was enriched using a bacterial mRNA purification kit (Dynabeads™, Thermo Fisher Scientific Inc). The purified mRNA was then mixed with a specialized fragmentation buffer to induce mRNA fragmentation. These fragmented mRNA molecules served as templates for first-strand cDNA synthesis using reverse transcriptase and random hexamer primers. Subsequently, the second-strand cDNA was synthesized by adding the appropriate buffer,

dNTPs, RNase H, and DNA polymerase I, resulting in the formation of double-stranded cDNA. The cDNA fragments then underwent end repair and A-tailing to facilitate the ligation of sequencing adapters. Size selection of the ligated cDNA was performed using agarose gel electrophoresis in nucleic acid electrophoresis apparatus (EPS-100, Shanghai Tanon Science & Technology Co.,Ltd.), and fragments of approximately (200 ± 25) bp were recovered. Finally, the selected cDNA fragments were amplified via Real-Time Quantitative PCR (qPCR) system (ABI Q7, Thermo Fisher Scientific Inc.) to construct the RNA-seq library, preparing the samples for subsequent high-throughput sequencing analysis.

2.6 RNA-seq high-throughput sequencing

High-throughput paired-end sequencing of the constructed RNA-seq libraries was performed on the Illumina HiSeq™ 4000 platform, aiming to comprehensively capture cDNA sequence information and ensure detailed data acquisition from both ends of the fragments. During the sequencing process, the raw image data were generated and subsequently processed through the base-calling pipeline to convert the images into raw sequencing reads. RNA extraction, cDNA synthesis, and RNA-seq were performed for three independent biological replicates per treatment group (n=3), and each replicate consisted of a single measurement.

2.7 Sequencing data filtering

Strict quality control procedures were applied to the raw sequencing data to ensure the accuracy of the results. The quality control process included three major steps: first, removal of low-quality reads to improve overall data quality; second, elimination of reads containing adapter sequences to reduce background noise; and third, filtering out reads with more than 5% unknown nucleotides (N) to ensure high data integrity. After these processing steps, high-quality clean reads were obtained for downstream analysis. To comprehensively assess the quality of the sequencing data, the ribosomal RNA (rRNA) content and the alignment to the reference genome were examined. Additionally, sequencing saturation and randomness were analyzed to evaluate the reliability and representativeness of the RNA-seq data.

2.8 Bioinformatics analysis

The gene expression data obtained from the RNA-seq were subjected to a comprehensive analysis of sample interactions using Pearson correlation coefficients and other statistical methods to evaluate the reproducibility among biological replicates. Based on these results, differential gene expression analysis between experimental groups was conducted using the edgeR software package. Strict filtering criteria were applied to identify significantly DEGs, defined as those with a false discovery rate (FDR) ≤ 0.001 and a fold change ≥ 2. The identified DEGs were subsequently annotated and functionally categorized through Gene Ontology (GO) enrichment analysis and Kyoto Encyclopedia of Genes and Genomes (KEGG) pathway analysis, to gain insights into their potential biological significance and involvement in cellular metabolic pathways. GO and KEGG enrichment analyses were performed using the clusterProfiler R package. DEGs with an adjusted P-value < 0.05 were used as input for the enrichment analysis. The significance threshold

for GO and KEGG terms was set to *P*-value < 0.05. For KEGG analysis, pathways were considered significant if they were enriched with at least 10 DEGs.

2.9 Validation by Real-Time Quantitative PCR (qRT-PCR)

Total RNA was extracted from *E. coli* O157:H7 samples from both the control group and the group subjected to combined US and UV treatment. The extracted RNA was reverse-transcribed into cDNA using a BIOG cDNA synthesis kit which served as the template for subsequent PCR amplification. The qPCR reaction mixture was prepared by combining the synthesized cDNA, gene-specific primers, BIOG^{HC} Elitefast SYBR kit (containing necessary enzymes and fluorescent dye), and nuclease-free water. The reactions were performed on a qRT-PCR system using a two-step amplification protocol. The thermal cycling conditions were set as follows: an initial denaturation at 95 ℃ for 10 minutes, followed by 40 cycles of amplification consisting of denaturation at 95 ℃ for 15 seconds and annealing/extension at 63 ℃ for 30 seconds. Fluorescence signals were collected at the end of each extension phase to monitor amplification in real time. Upon completion of the PCR cycles, a melting curve analysis was conducted to assess the specificity of the PCR products. The relative expression levels of target genes were calculated and compared with the RNA-seq results for validation. The primer sequences used for the randomly selected DEGs were listed in Table 1.

Table 1 Target gene primer sequence

Gene Name	Primer Sequences (5' to 3')
frdD	ATGATTAATCCAAATCCAAA TTGGTGTCGTTACAATCTAA
holB	ATGAGATGGTATCCATGGTT TACCGGTTCCTCATCTTTAA
LsrC	ATGCTGAAGTTTATTCAGAA AAAACGGGAGGCTGCATAA
agaC	ATGCATGAAATAACCCTACT ACTACAGCAATGGGATCTGA
rplK	ATGGCTAAGAAAGTACAAGC GCCTGGTAGTGGAGGACTAA
fepB	GTGAGACTCGCCCCGCTCTA GACTTAAGGCGCTGTTTTAA

3. Results and Discussions

Following quality control of the raw sequencing data, high-quality reads were obtained, with Q20 values exceeding 97% and Q30 values around 94%, ensuring data reliability for downstream analyses. Under stringent screening criteria (FDR ≤ 0.001, fold change ≥ 2), a total of 2,133 differentially expressed genes (DEGs) were identified in *E. coli* O157:H7 following combined US+UV treatment, including 1,055 up-regulated and 1,078 down-regulated genes (Figure 2). Gene Ontology (GO) annotation analysis revealed that these DEGs were primarily involved in biological processes such as carbohydrate metabolism, bioadhesion, lipid metabolism, and protein hydrolysis. They were associated with cellular components such as fimbriae, cytoplasmic membranes, and ATPase complexes, and were enriched in molecular functions related to catalysis, binding, and transport activity. KEGG pathway analysis further classified these DEGs

into five major functional categories: metabolism, genetic information processing, environmental information processing, cellular processes, and organismal systems. Notably, key pathways affected included carbon metabolism, amino acid biosynthesis, transcription and translation, membrane structure, oxidative phosphorylation, and quorum sensing, providing molecular insights into the complex cellular responses and damage mechanisms induced by the US+UV combined treatment.

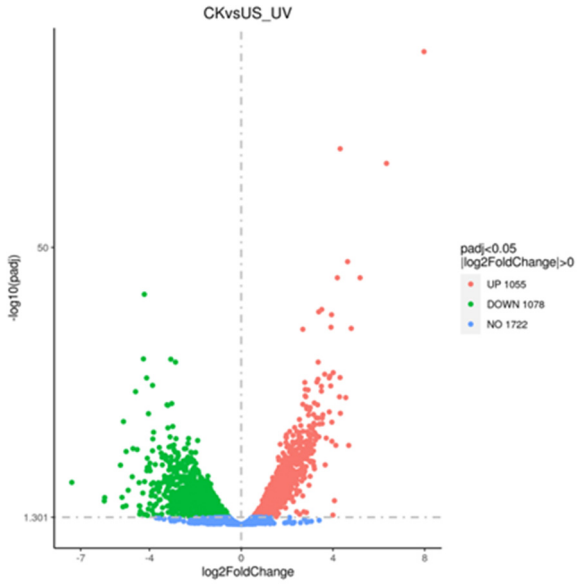

Fig.2 Volcano map of gene expression correlation.

3.1 Transport and metabolism of carbohydrates

As a unique energy-dependent sugar transport mechanism, the phosphotransferase system (PTS) in bacteria enabled the simultaneous phosphorylation of sugar molecules during their translocation across the membrane. This system involved complex protein–protein interactions and a series of sequential catalytic reactions. The PTS comprised three major components: the universally conserved enzyme I (EI) and histidine-containing phosphocarrier protein (HPr), as well as the sugar-specific enzyme II (EII) complex, which was further subdivided into the IIAB, IIC, and IID subunits. In *E. coli* O157:H7, more than twenty EII proteins were genome-encoded, exhibiting high substrate specificity and being primarily responsible for the efficient transport and phosphorylation of various carbohydrates[12].

Table 2 presented the expression profiles of the genes relevant to the PTS in *E. coli* O157:H7 following US+UV treatment. Notably, the *ptsI* gene, encoding a general component of the system, was significantly up-regulated, indicating an enhanced capacity for energy-dependent sugar transport. In contrast, genes encoding substrate-specific components showed down-regulated expression. For instance, the decreased expression of *agaC* and *agaD* suggested a reduction in the activity of the EIIC components involved in galactosamine transport, potentially slowing its intracellular uptake. Similarly, the down-regulation of *celA* and *celC* indicated impaired activity of the EIIB components responsible for cellobiose transport, which might have negatively impacted cell wall structure and stability. Additionally, down-regulation of *UlaA* and *UlaC* implied reduced intracellular distribution of L-ascorbate, potentially affecting the bacterium's antioxidant capacity and energy metabolism. These findings indicated that US+UV treatment significantly

altered the expression of carbohydrate metabolism-related genes in *E. coli* O157:H7. Up-regulation of certain genes might have reflected an adaptive response aimed at maintaining nutrient supply under stress, whereas down-regulation of others likely pointed to detrimental effects on cellular structure and metabolic functions[13].

Table 2 Differentially expressed genes in the PTS

Gene ID	Gene Name	Fold Change	Gene Expression Product
I6L76_RS00295	ptsI	0.94	phosphoenolpyruvate-protein phosphotransferase (PTS system enzyme I)
I6L76_RS19030	agaC	-1.74	galactosamine PTS system EIIC component
I6L76_RS19025	agaD	-0.95	galactosamine PTS system EIID component
I6L76_RS15395	celA	-5.02	cellobiose PTS system EIIB component
I6L76_RS15410	celC	-2.27	cellobiose PTS system EIIA component
I6L76_RS00730	UlaA	-1.66	ascorbate PTS system EIIC component
I6L76_RS00720	UlaC	-1.83	ascorbate PTS system EIIA or EIIAB component

The tricarboxylic acid cycle (TCA), alternatively termed the citric acid or Krebs cycle, described a cyclic metabolic pathway functioning within cells. Under aerobic conditions, it occurred in the mitochondria (in eukaryotes) or the cytoplasm (in prokaryotes). The TCA cycle served as a key pathway in the oxidative catabolism of organic substrates, particularly carbohydrates, fats, and proteins, producing metabolic intermediates[14]. The primary function of the TCA cycle was to release the energy stored in organic molecules, facilitating the transfer of energy and electrons, and the production of high-energy compounds. Several steps in the TCA cycle involved the transfer of hydrogen atoms and electrons, which were then conveyed through the electron transport chain to drive ATP synthesis. The high-energy compounds produced, such as ATP, NADH, and FADH2, served as energy-rich molecules for various cellular metabolic activities[15].

Table 3 illustrated that the genes associated with enzymes involved in the TCA cycle were predominantly up-regulated, including *sucA*, *sucC*, *sucD*, *ydbK*, *frdD*, and *frdB*. *sucA* encoded the E1 component of the 2-oxoglutarate dehydrogenase complex, which played a role in the TCA cycle, and its up-regulation suggested an increase in TCA cycle activity. The genes *sucC* and *sucD* encoded the two subunits of succinyl-CoA synthetase, which catalyzed the conversion of succinate to succinyl-CoA, a key step in the cycle, and ATP production. Their up-regulation implied enhanced ATP activity in the cell. Additionally, *ydbK* was involved in the metabolism of pyruvate under anaerobic conditions, while *frdD* and *frdB* were involved in the oxidation of succinate to fumarate, with their up-regulation reflecting changes in cellular oxidative stress or energy metabolism. Recent studies demonstrated that combined ultrasound and UV treatment could markedly enhance intracellular reactive oxygen species (ROS) generation in *E. coli* O157:H7, leading to oxidative damage of cellular components and disruption of redox homeostasis [7]. Elevated ROS levels could stimulate metabolic reprogramming to meet the increased energy demand for stress adaptation. Consistent with this, our US+UV transcriptomic data showed up-regulation of multiple TCA-cycle and oxidative phosphorylation genes (e.g., f*rdD*, *frdB*, *sucA*, *nuoM*), suggesting enhanced ATP

production potentially linked to ROS-induced stress responses. Similar ROS-mediated metabolic shifts were observed under high-intensity ultrasound, which triggered apoptosis-like death with ROS accumulation and ATP depletion, and under UV irradiation, which induced oxidative damage and modulated central carbon metabolism.

Table 3 Differentially expressed genes in the TCA

Gene ID	Gene Name	Fold Change	Gene Expression Product
I6L76_RS00720	sucA	1.16	2-oxoglutarate dehydrogenase E1 component
I6L76_RS00720	sucC	1.03	succinyl-CoA synthetase alpha subunit
I6L76_RS00720	sucD	1.18	succinyl-CoA synthetase beta subunit
I6L76_RS04005	ydbK	2.69	pyruvate-ferredoxin/flavodoxin oxidoreductase
I6L76_RS13575	frdD	1.98	succinate dehydrogenase subunit D
I6L76_RS13565	frdB	1.73	succinate dehydrogenase iron-sulfur subunit

Interestingly, the apparent co-up-regulation of both *suc* genes (aerobic metabolism) and *frd* genes (anaerobic metabolism) might reflect a metabolic flexibility that allowed the bacterium to maximize ATP production by engaging both aerobic respiration and anaerobic electron transport under US+UV stress. Such dual activation could be an adaptive strategy to maintain energy homeostasis in response to oxidative and structural stress. In contrast to our findings, Wei et al.[16] observed a down-regulation of TCA cycle-related protein expression in *Bacillus subtilis* under high-frequency ultrasound treatment, alongside an up-regulation of proteins related to oxidative phosphorylation. These findings suggested that different bacterial species exhibited distinct differences in their carbohydrate transport and metabolism processes when subjected to environmental stress treatments.

3.2 Amino acid biosynthesis and metabolism

Amino acids constituted the core components of proteins and were crucial organic molecules for cellular and organismal viability. They played vital roles in protein synthesis, energy production, metabolic regulation, biosynthetic processes, and the maintenance of cellular acid-base balance. Therefore, the production, degradation, and regulatory mechanisms of amino acids were focal points in cellular biology and omics research.

As shown in Table 4, most genes involved in the biosynthesis of valine, leucine, and isoleucine were up-regulated following the combined US and UV treatment. These three branched-chain amino acids (BCAAs) were closely linked in their biosynthetic pathways and shared common initial steps. The synthesis began with pyrophosphate pyridoxal and α-ketoglutarate, where pyrophosphate pyridoxal was first converted into a 2-keto acid. This intermediate was then catalyzed by acetolactate synthase into either 2-acetolactate or 2-aceto-2-hydroxybutyrate. 2-Acetolactate was subsequently converted into 2,3-dihydroxy-isovalerate through the action of decarboxylase. For valine, 2,3-dihydroxy-isovalerate underwent further reactions, such as decarboxylation and transamination, to yield valine. For leucine, 2-acetolactate was transformed into 2-isopentenate, which was then converted to leucine. For isoleucine, 2-aceto-2-hydroxybutyrate proceeded through a series of steps to form isoleucine. Notably, the genes *leuA* and l*euB* (involved in leucine biosynthesis), *leuC* and *leuD* (for isoleucine biosynthesis), and *ilvD* (for valine

biosynthesis) were significantly up-regulated. The branched-chain amino acid transaminase gene *ilvE*, which catalyzed the final step by transferring an amino group to the corresponding α-keto acid to form the respective amino acid, was also up-regulated, indicating enhanced amino acid metabolic activity[17].

Table 4 Differentially expressed genes in amino acid synthesis metabolism

Gene ID	Gene Name	Fold Change	Gene Expression Product
I6L76_RS12065	leuA	2.02	2-isopropylmalate synthase
I6L76_RS12070	leuB	1.84	3-isopropylmalate dehydrogenase
I6L76_RS12075	leuC	1.55	3-isopropylmalate/(R)-2-methylmalate dehydratase large subunit
I6L76_RS12080	leuD	1.17	3-isopropylmalate/(R)-2-methylmalate dehydratase small subunit
I6L76_RS16590	ilvD	1.54	dihydroxy-acid dehydratase
I6L76_RS16585	ilvE	2.14	branched-chain amino acid aminotransferase

Based on the table data, it could be inferred that the combined US and UV treatment activated the branched-chain amino acid biosynthesis pathways in *E. coli* O157:H7. This likely represented a bacterial stress response aimed at repairing damaged cellular structures or enhancing resistance to environmental pressure. Previous studies also showed that multiple metabolic pathways, including amino acid and glutamate metabolism, were significantly altered in *E. coli* under ultrasound treatment[18]. Given their crucial roles in protein synthesis, energy metabolism, and metabolic regulation, the up-regulation of BCAAs might have assisted bacteria in recovery and adaptation under stress. Additionally, the enhanced synthesis of BCAAs could have been associated with changes in bacterial intracellular signal transduction, which were known to play roles in stress resistance and survival mechanisms.

3.3 Transcription- and translation-related functions

DNA replication within *E. coli* O157:H7 exhibited remarkable precision, enabling accurate inheritance of genetic material during division. This process included the incorporation of deoxyribonucleotides (dNTPs), bidirectional replication, primer synthesis and removal, as well as correct base pairing[19]. According to the gene expression data presented in Table 5, the *holB* and *holC* genes were found to be up-regulated. These genes encoded the δ and χ subunits of DNA polymerase III, respectively, which was the main enzyme responsible for DNA replication in *E. coli* O157:H7. The up-regulation of these subunits suggested that the cells were enhancing their DNA replication capacity, possibly as a compensatory response to DNA damage induced by US and UV treatment. Additionally, the *lig* gene, which encoded DNA ligase, was also up-regulated. DNA ligase played a critical role in sealing nicks in the DNA backbone, essential during both DNA repair and replication. The increased activity of this enzyme might have indicated an enhanced effort by the cells to repair potential DNA strand breaks. This finding was consistent with the study by Wang et al.[20], which demonstrated that UV irradiation could disrupt normal DNA synthesis and thereby inactivate bacterial cells. Overall, the up-regulation of these genes suggested that *E. coli* O157:H7 activated adaptive mechanisms triggered by DNA damage caused by the combined US and UV treatment. This included reinforcement of the DNA repair and replication machinery to preserve genetic integrity and stability. These results implied that the treatment might have triggered cellular stress responses and activated DNA damage repair pathways.

Table 5 Differentially expressed genes related to DNA replication

Gene ID	Gene Name	Fold Change	Gene Expression Product
I6L76_RS06835	holB	1.42	DNA polymerase III subunit delta'
I6L76_RS18670	holC	1.49	DNA polymerase III subunit chi
I6L76_RS14945	lig	1.69	DNA ligase (NAD+)

Ribosomes were essential organelles within cells responsible for protein synthesis. Ribosomes, which contained both rRNA and ribosomal proteins, were essential for translating mRNA into protein-coding amino acid sequences. This vital cellular machinery comprised two subunits: the 50S large subunit and the 30S small subunit. Each subunit contained multiple ribosomal proteins and rRNA molecules that cooperated in the translation process[19].

As shown in Table 6, following the combined US and UV treatment, the expression of several genes encoding components of both ribosomal subunits—including *rpsF*, *rpsR*, *rplK*, *rplA*, *rpmB*, and *rpsT*—was significantly down-regulated compared to untreated cells. This reduction in gene expression might have impaired ribosome assembly and function, consequently leading to diminished protein synthesis capacity in the cells. This observation also suggested that the cells were likely undergoing a stress response, reallocating energy and resources toward essential survival processes—such as DNA repair and membrane integrity maintenance—rather than growth and proliferation. This was consistent with the observed up-regulation of DNA replication-related genes, indicating a shift in cellular priorities due to treatment-induced stress. Overall, these results demonstrated that the combined US and UV treatment significantly altered the physiological state of *E. coli* O157:H7, suppressing its growth and protein production capabilities.

Table 6 Differentially expressed genes encoded by ribosomes

Gene ID	Gene Name	Fold Change	Gene Expression Product
I6L76_RS13405	rpsF	-2.02	small subunit ribosomal protein S6
I6L76_RS13395	rpsR	-1.25	small subunit ribosomal protein S18
I6L76_RS14320	rplK	-2.16	large subunit ribosomal protein L11
I6L76_RS14315	rplA	-1.53	large subunit ribosomal protein L1
I6L76_RS14810	rpmB	-2.08	large subunit ribosomal protein L28
I6L76_RS12265	rpsT	-1.81	small subunit ribosomal protein S20

3.4 Cell wall and membrane-associated functions

The outer membrane of *E. coli* O157:H7, composed of lipopolysaccharides (LPS) and a peptidoglycan layer, constituted the primary structure of its cell wall. LPS alone covered approximately three-quarters of the cell surface and consisted of lipid A (which exhibited endotoxin activity), a core oligosaccharide, and an O-specific polysaccharide[21]. According to Table 7, the genes *lpxA* and *lpxC*, which encoded UDP-N-acetylglucosamine acyltransferase, were significantly up-regulated following US combined with UV treatment. This up-regulation might have indicated enhanced cell wall biosynthesis, representing a potential adaptive response by *E. coli* O157:H7 to strengthen its structural integrity under external stress, thereby protecting the cell from damage. In Gram-negative bacteria, LPS in the outer membrane played a crucial role in both immune recognition and environmental sensing. For *E. coli* O157:H7, LPS was not only

essential for virulence but also a key determinant of environmental adaptability. In addition to LPS, the outer membrane contained proteins and phospholipids that collectively formed the interface between the bacterium and its surroundings. In our results, genes closely associated with LPS structure, such as *crcA* and *ddg*, exhibited a downward trend in expression, which might have reflected membrane damage induced by the combined US and UV treatment, thereby disrupting the expression of these structural genes.

Table 7 Differentially expressed genes related to cell wall and membrane

Gene ID	Gene Name	Fold Change	Gene Expression Product
I6L76_RS11580	lpxA	1.47	UDP-N-acetylglucosamine acyltransferase
I6L76_RS11960	lpxC	1.62	UDP-3-O-[3-hydroxymyristoyl] N-acetylglucosamine deacetylase
I6L76_RS14785	kdtA	-1.13	3-deoxy-D-manno-octulosonic-acid transferase
I6L76_RS09440	crcA	-1.88	lipid IVA palmitoyltransferase
I6L76_RS00455	ddg	-1.43	KDO2-lipid IV(A) palmitoleoyltransferase

Furthermore, ATP-binding cassette (ABC) transporters, which played vital roles in membrane-associated transport functions, were also affected. These transport proteins, embedded in the cytoplasmic membrane of *E. coli* O157:H7, typically consisted of two ATP-binding domains and utilized ATP hydrolysis to mediate substrate translocation across the membrane. ABC transporters in this organism were responsible for both nutrient uptake and waste efflux, with substrate specificity for polysaccharides, amino acids, peptides, and other molecules, thereby playing a critical role in bacterial physiology[22]. Table 8 showed that most genes related to membrane transport were down-regulated after the combined treatment, including *cysP* and *sbp* (involved in inorganic and organic ion transport), *ycjV* and *malK* (for oligosaccharide, polyol, and lipid transport), *ugpA* and *ugpE* (for monosaccharide transport), *fepB* and *yadT* (for metal cation, iron oxide, and vitamin B12 transport), and *phnE*, *artJ*, and *abc* (involved in phosphate and amino acid transport). These observations suggested that US and UV treatment compromised not only the integrity of the cell membrane but also impaired its transport capacity. These findings were consistent with those of Bai et al.[23], who reported that both US and UV treatment interfered with ABC transporter synthesis, disrupting membrane permeability and ion exchange channels.

Table 8 Differentially expressed genes related to ABC transporter proteins

Gene ID	Gene Name	Fold Change	Gene Expression Product
I6L76_RS00260	cysP	-2.13	sulfate/thiosulfate transport system substrate-binding protein
I6L76_RS16335	sbp	-1.40	sulfate/thiosulfate transport system substrate-binding protein
I6L76_RS04325	ycjV	-3.22	multiple sugar transport system ATP-binding protein
I6L76_RS03890	malK	-2.07	multiple sugar transport system ATP-binding protein
I6L76_RS17465	ugpA	-1.82	sn-glycerol 3-phosphate transport system permease protein
I6L76_RS17470	ugpE	-1.64	sn-glycerol 3-phosphate transport system permease protein
I6L76_RS09630	fepB	-3.20	ferric enterobactin transport system substrate-binding protein
I6L76_RS11685	yadT	-1.05	vitamin B12 transport system substrate-binding protein
I6L76_RS13750	phnE	-3.99	phosphonate transport system permease protein
I6L76_RS05915	artJ	-1.87	arginine transport system substrate-binding protein
I6L76_RS10115	abc	-2.47	D-methionine transport system ATP-binding protein

3.5 Oxidative respiratory chain

Oxidative phosphorylation was a key process in cellular respiration. Under aerobic conditions, *E. coli* O157:H7 could generate energy through oxidative phosphorylation. This process primarily took place on the cytoplasmic membrane, where NADH and $FADH_2$—generated from glycolysis, pyruvate oxidation, and the tricarboxylic acid (TCA) cycle—served as high-energy electron donors for the electron transport chain (ETC). These electrons were transferred to oxygen via a series of membrane-associated protein complexes, including NADH dehydrogenase, cytochrome b/c complex, and cytochrome oxidase. The components of the ETC in *E. coli* O157:H7 might have differed slightly from those in eukaryotic organisms, as the bacterium possessed multiple types of dehydrogenases and oxidases that could be modulated based on environmental conditions. During electron transfer, complexes I, III, and IV translocated protons from the cytoplasm to the periplasmic space, generating a proton motive force composed of a proton gradient and membrane potential. This proton motive force drove protons back into the cytoplasm via the ATP synthase complex (F_0F_1-type ATP synthase), which catalyzed the phosphorylation of ADP with inorganic phosphate (Pi) to form ATP[24].

As shown in Table 9, the expression of the genes involved in the electron-transport chain increased following the combined US and UV treatment. The nuoC and nuoE genes produced subunits of NADH: quinone oxidoreductase (Complex I), an enzyme complex that facilitated electron transfer from NADH to quinone while simultaneously driving proton translocation across the membrane to generate a proton gradient. This gradient provided the electrochemical potential necessary for ATP production. The frdD and frdC genes coded for components of succinate dehydrogenase (Complex II), which catalyzed the conversion of succinate to fumarate within the TCA cycle and channeled electrons to quinone. Additionally, the ppk gene encoded polyphosphate kinase, an enzyme involved in energy regulation and ATP formation. Similarly, Wei et al.[16] reported that high-intensity ultrasound treatment led to the up-regulation of many oxidative phosphorylation-related proteins in Bacillus subtilis, indicating that ultrasound might have promoted increased ATP production. Collectively, these gene expression changes suggested that E. coli O157:H7 might have enhanced respiratory chain activity following combined US and UV exposure to generate more energy, allowing the cell to respond to and adapt to the imposed environmental stress. This was consistent with the previously observed up-regulation of the TCA cycle pathway.

Table 9 Differentially expressed genes in the oxidative respiratory chain

Gene ID	Gene Name	Fold Change	Gene Expression Product
I6L76_RS00805	nuoC	0.96	NADH-quinone oxidoreductase subunit C/D
I6L76_RS00810	nuoE	1.25	NADH-quinone oxidoreductase subunit E
I6L76_RS00850	nuoM	2.43	NADH-quinone oxidoreductase subunit M
6L76_RS13565	frdB	1.73	succinate dehydrogenase iron-sulfur subunit
6L76_RS13570	frdC	1.62	succinate dehydrogenase subunit C
6L76_RS13575	frdD	1.98	succinate dehydrogenase subunit D
6L76_RS00040	ppk	1.01	polyphosphate kinase

3.6 Quorum sensing

Quorum sensing (QS) referred to a bacterial communication system that regulated group activities through the production and recognition of specific signaling molecules. This system allowed the bacteria to assess their population density and coordinate collective actions, which were essential for controlling processes like biofilm development, virulence expression, antibiotic generation, and resistance mechanisms. Autoinducer-2 (AI-2), a widely conserved signaling molecule among bacterial species, participated in a complex QS regulatory mechanism. AI-2 first bound to *LsrB*, then entered the cell via a transmembrane channel formed by *LsrC* and *LsrD*, a process that required ATP hydrolysis by *LsrA* to provide energy. Once inside the cell, AI-2 was phosphorylated by *LsrK* and subsequently processed by *LsrF* and *LsrG*. The phosphorylated AI-2 interacted with the repressor protein *LsrR*, relieving its inhibition and initiating transcription of the *lsr* operon, thus completing the signal transduction process. Following combined US and UV treatment, the expression of QS-related genes was observed to be up-regulated (Table 10). This suggested that the bacteria might have enhanced their quorum sensing capabilities in response to environmental stress, potentially increasing biofilm formation via QS regulation as a defensive strategy. Previous studies showed that QS activity in *E. coli* O157:H7 was suppressed under ultrasound treatment alone[18], indicating that the combined stress of US and UV might have triggered different cellular responses. It was possible that the dual stress altered the bacterial response to ultrasound by affecting DNA repair systems or intracellular signaling pathways, thereby indirectly enhancing the activity of the QS system. In addition, the *dpp* gene, which was responsible for transporting specific peptides, was found to be down-regulated. This indicated a reduction in peptide uptake and transport, possibly reflecting metabolic adjustments under environmental stress or damage to membrane function caused by the combined treatment. Such damage could impair nutrient uptake and overall bacterial viability. These differential gene expression patterns further suggested that *E. coli* O157:H7 adapted to and resisted combined US and UV treatment by modulating its gene expression profile.

Table 10 Differentially expressed genes related to QS

Gene ID	Gene Name	Fold Change	Gene Expression Product
I6L76_RS19270	LsrB	1.72	AI-2 transport system substrate-binding protein
I6L76_RS19260	LsrC	1.84	AI-2 transport system permease protein
I6L76_RS19245	LsrK	1.47	autoinducer-2 kinase
I6L76_RS19280	LsrG	1.21	(4S)-4-hydroxy-5-phosphonooxypentane-2,3-dione isomerase
I6L76_RS01615	Dpp	-1.51	peptide/nickel transport system ATP-binding protein

To evaluate whether the US+UV treatment elicited transcriptomic changes distinct from those of single treatments, we compared our DEGs with published datasets of *E. coli* exposed to ultrasound alone or UV/light emitting diode (LED) irradiation. Several stress-response pathways, including carbohydrate metabolism, membrane transport systems (ABC transporters, PTS), and oxidative stress defense, were commonly regulated across studies, indicating shared cellular responses to physical stress. However, notable differences were observed. Li et al. [25] and Wang et al. [26] reported that ultrasound alone generally

down-regulated TCA cycle and oxidative phosphorylation genes, whereas our US+UV dataset showed up-regulation of multiple genes in these pathways (e.g., *frdB*, *frdD*, *sucA*, *nuoM*), suggesting enhanced ATP production under combined stress. In addition, the US+UV treatment concurrently down-regulated ribosomal protein genes and ABC transporter genes while upregulating the *lsr* quorum-sensing operon, a pattern that was absent in both ultrasound-only and UV/LED-only treatments. Khan et al.[27] observed limited or no induction of *lsr* genes under LED exposure. These comparisons indicated that US+UV triggered a transcriptional program that included both shared stress responses and distinct features not explained by the simple additive effects of single treatments, potentially reflecting synergistic cellular adaptation to dual physical stresses.

3.7 Validation by qPCR

To ensure the reliability of transcriptome-based differential gene expression data, several *E. coli* O157:H7 genes subjected to combined US and UV treatment were randomly selected for qPCR validation. As shown in Table 11, genes such as *frdD*, *holB*, *LsrC*, *agaC*, *rplK*, and *fepB* exhibited expression trends (either up-regulation or down-regulation) consistent with the RNA-seq data. This consistency confirmed the high accuracy and reliability of the RNA-seq results.

Table 11 qPCR validation of differentially expressed genes

Gene Name	Gene Expression Product	qPCR Fold Change	Trend	RNA-seq Fold Change	Trend
frdD	succinate dehydrogenase subunit D	1.53	Up-regulated	1.98	Up-regulated
holB	DNA polymerase III subunit delta'	1.25	Up-regulated	1.42	Up-regulated
LsrC	AI-2 transport system permease protein	1.34	Up-regulated	1.84	Up-regulated
agaC	galactosamine PTS system EIIC component	-1.53	Down-regulated	-1.74	Down-regulated
rplK	large subunit ribosomal protein L11	-1.72	Down-regulated	-2.16	Down-regulated
fepB	ferric enterobactin transport system substrate-binding protein	-1.64	Down-regulated	-3.20	Down-regulated

4. Conclusions

This study was the first to employ high-throughput RNA-seq to systematically profile transcriptomic responses of *E. coli O157:H7* to simultaneous ultrasound and ultraviolet (US+UV) treatment, revealing novel molecular insights into its synergistic bactericidal mechanism. The combined treatment triggered coordinated regulation across multiple critical pathways, including up-regulation of TCA cycle and oxidative phosphorylation genes to enhance ATP generation, down-regulation of ribosomal and ABC transporter genes to suppress protein synthesis and impair membrane transport, and activation of AI-2–mediated quorum sensing potentially linked to collective stress adaptation. These results suggested that US+UV achieved microbial inactivation via a multi-target mode of action, simultaneously disrupting cellular energy balance, structural integrity, and communication networks (Fig. 3).

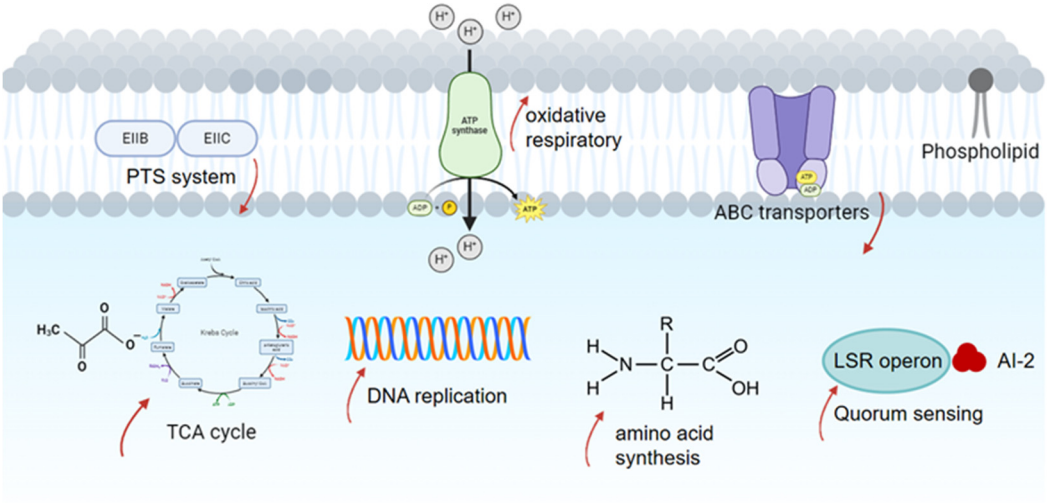

Fig.3 Schematic diagram of the effects of ultrasound combined with ultraviolet treatment on the main metabolic pathways of *E. coli* O157:H7(arrows indicated up-regulation or down-regulation of differentially expressed genes).

However, this study had limitations. All measurements were taken at a single time point (40 s), preventing distinction between immediate and long-term responses. Future work will include multi-time-point transcriptomic analyses, combined with proteomic, metabolomic, and in situ validation in food matrices, to further elucidate the mechanism and optimize US+UV applications.

Declaration of Competing Interest

The authors declare that they have no known competing financial interests or personal relationships that could have appeared to influence the work reported in this paper.

References

[1] Chemat F, Zill-e-Huma, Khan M K. Applications of ultrasonic in food technology: Processing, preservation and extraction, Ultrason Sonochem 18 (2011) 813–835. http://dx.doi.org/10.1016/j.ultsonch.2010.11.023.

[2] Zupanc M, Pandur Ž, Perdih T S, et al. Effects of cavitation on different microorganisms: The current understanding of the mechanisms taking place behind the phenomenon. A review and proposals for further research, Ultrason Sonochem 57 (2019) 147–165. http://dx.doi.org/10.1016/j.ultsonch.2019.05.009.

[3] Piyasena P, Mohareb E, McKellar R C. Inactivation of microbes using ultrasound: a review, Int J Food Microbiol 87 (2003) 207–216. http://dx.doi.org/10.1016/S0168-1605(03)00075-8.

[4] Li X, Farid M. A review on recent development in non-conventional food sterilization technologies, J Food Eng 182 (2016) 33–45. http://dx.doi.org/10.1016/j.jfoodeng.2016.02.026.

[5] Gratz M, Sevenich R, Hoppe T, et al. Gentle sterilization of carrot-based purees by high-pressure thermal sterilization and ohmic heating and influence on food processing contaminants and quality attributes, Front Nutr 8 (2021) 643837. http://dx.doi.org/10.3389/fnut.2021.643837.

[6] Jin H, Dong B, Sun Y, Lei Z. Synergistic efficiency of *E. coli* inactivation under US and UV, Environ Sci Technol 33 (2010). http://dx.doi.org/10.3969/j.issn.1003-6504.2010.11.005.

[7] Chen Y, Wu Y H, Zhou J W, et al. Bactericidal effect and mechanism of ultrasound combined with ultraviolet treatment on *Escherichia coli* O157:H7, Food Sci (2025) 1-13.

[8] Hummert M, Leenders P, Mellmann A, et al. Generation of plasma-activated fluids for successful disinfection of *Pseudomonas aeruginosa* in liquid environments and determination of microbial damage, Plasma 6 (2023) 699–713. http://dx.doi.org/10.3390/plasma6040048.

[9] Wen Q. Antibacterial mechanism of thymol based on cell membrane, metabolomic and transcriptomic properties of food-borne pathogen, South China University of Technology (2022).

[10] Al-Jassim N, Mantilla-Calderon D, Wang T, Hong P. Inactivation and gene expression of a virulent wastewater *Escherichia coli* strain and the nonvirulent commensal *E. coli* DSM1103 strain upon solar irradiation, Environ Sci Technol 51 (2017) 3649–3659. http://dx.doi.org/10.1021/acs.est.6b05377.

[11] Zhao F, Wang Y, An H, et al. New insights into the formation of viable but nonculturable *Escherichia coli* O157:H7 induced by high-pressure CO_2, mBio 7 (2016) e00961-16. http://dx.doi.org/10.1128/mBio.00961-16.

[12] Lei J, Li L, Su X. Crystal structures of phosphotransferase system enzymes PtxB (IIB^{Asc}) and PtxA (IIA^{Asc}) from *Streptococcus mutans*, J Mol Biol 386 (2009) 465–475. http://dx.doi.org/10.1016/j.jmb.2008.12.046.

[13] Steen J A, Bohlke N, Vickers C E, et al. The trehalose phosphotransferase system (PTS) in *E. coli* W can transport low levels of sucrose that are sufficient to facilitate induction of the *csc* sucrose catabolism operon, PLOS ONE 9 (2014) e88688. http://dx.doi.org/10.1371/journal.pone.0088688.

[14] Baldwin J E, K H. The evolution of metabolic cycles, Nature 291 (1981) 381–382. http://dx.doi.org/10.1038/291381a0.

[15] Nguyen T T, Torrini C, Shang E, et al. OGDH and Bcl-xL loss causes synthetic lethality in glioblastoma, JCI Insight 9 (2024) e172565. http://dx.doi.org/10.1172/jci.insight.172565.

[16] Luo W, Wang J, Wang Y, et al. Bacteriostatic effects of high-intensity ultrasonic treatment on *Bacillus subtilis* vegetative cells, Ultrason Sonochem 81 (2021) 105862. http://dx.doi.org/10.1016/j.ultsonch.2021.105862.

[17] Keefe A D, Lazcano A, Miller S L. Evolution of the biosynthesis of the branched-chain amino acids, Orig Life Evol Biosph 25 (1995) 99–110. http://dx.doi.org/10.1007/BF01581576.

[18] Li J, Liu D, Ding T. Transcriptomic analysis reveal differential gene expressions of *Escherichia coli* O157:H7 under ultrasonic stress, Ultrason Sonochem 71 (2021) 105418. http://dx.doi.org/10.1016/j.ultsonch.2020.105418.

[19] Burkhardt N, Diedrich G, Nierhaus K H, et al. Architecture of the *E. coli* 70S ribosome, Physica B 234 (1997) 199–201.

[20] Wang J, Qu D, Bu L, Zhu S. Inactivation efficiency of *P. aeruginosa* and ARGs removal in UV/NH_2Cl process: Comparisons with UV and NH_2Cl, Sep Purif Technol 305 (2023) 122473. http://dx.doi.org/10.1016/j.seppur.2022.122473.

[21] Breazeale S D, Ribeiro A A, McClerren A L, Raetz C R H. A formyltransferase required for polymyxin resistance in *Escherichia coli* and the modification of lipid A with 4-amino-4-deoxy-L-arabinose, J Biol Chem 280 (2005) 14154–14167. http://dx.doi.org/10.1074/jbc.M414265200.

[22] Young J, Holland I B. ABC transporters: bacterial exporters—revisited five years on, Biochim Biophys Acta Biomembr 1461 (1999) 177–200. http://dx.doi.org/10.1016/s0005-2736(99)00158-3.

[23] Bai Y, Zhou Y, Chang R, et al. Transcription profiles and phenotype reveal global response of *Staphylococcus aureus* exposed to ultrasound and ultraviolet stressors, Sci Total Environ 912 (2024) 169146. http://dx.doi.org/10.1016/j.scitotenv.2023.169146.

[24] Krah A. Linking structural features from mitochondrial and bacterial F-type ATP synthases to their distinct mechanisms of ATPase inhibition, Prog Biophys Mol Biol 119 (2015) 94–102. http://dx.doi.org/10.1016/j.pbiomolbio.2015.06.005.

[25] Li J, Liu D, Ding T. Transcriptomic analysis reveal differential gene expressions of *Escherichia coli* O157:H7 under ultrasonic stress, Ultrason Sonochem 71 (2021) 105418. http://dx.doi.org/10.1016/j.ultsonch.2020.105418.

[26] Wang X, Wang L, Ding T, Ye X, Liu D. *Escherichia coli* K-12 transcriptomics for assessing the mechanism of action of high-power ultrasound, Microorganisms 11 (2023) 2768. http://dx.doi.org/10.3390/microorganisms11112768.

[27] Khan S A, Kim H S, Kim D, et al. Genome-wide transcriptional response of *Escherichia coli* O157:H7 to light-emitting diodes with various wavelengths, Sci Rep 13 (2023) 1976. http://dx.doi.org/10.1038/s41598-023-28944-6.